Critical Heat Flux of Liquid Hydrogen, Liquid Methane, and Liquid Oxygen: A Review of Available Data and Predictive Tools

Michael Baldwin[1], Ali Ghavami[1], S. Mostafa Ghiaasiaan[1], Alok Majumdar[2]

[1]G.W. Woodruff School of Mechanical Engineering

Georgia Institute of Technology

Atlanta, Georgia 30332-0405

[2]Propulsion System Department

NASA/Marshall Space Flight Center

ABSTRACT

Available experimental data dealing with critical heat flux (CHF) of liquid hydrogen (LH2), liquid methane (LCH4), and liquid oxygen (LO2) in pool and flow boiling are compiled. The compiled data are compared with widely used correlations.

Experimental pool boiling CHF data for the aforementioned cryogens are scarce. Based on only 25 data points found in five independent sources, the correlation of Sun and Lienhard (1970) is recommended for predicting the pool CHF of LH2. Only two experiments with useful CHF data for the pool boiling of LCH4 could be found. Four different correlations including the correlation of Lurie and Noyes (1964) can predict the pool boiling CHF of LCH4 within a factor of two for more than 70% of the data. Furthermore, based on the 19 data points taken from only two available sources, the correlation of Sun and Lienhard (1970) is recommended for the prediction of pool CHF of LO2.

Flow boiling CHF data for LH2 could be found in seven experimental studies, five of them from the same source. Based on the 91 data points, it is suggested that the correlation of Katto and Ohno (1984) be used to predict the flow CHF of LH2. No useful data could be found for flow boiling CHF of LCH4 or LO2.

The available databases for flow boiling of LCH4 and LO2 are generally deficient in all boiling regimes. This deficiency is particularly serious with respect to flow boiling.

Notation

A = area
Bo = boiling number
Co = convection number
C_p= specific heat
D= diameter of disk or pipe
f= Darcy friction factor
G= mass flux
g= gravitational constant
h= heat transfer coefficient
$h_{fg} = h_g - h_f$ latent heat of vaporization
K_P = dimensionless parameter
k= thermal conductivity
L= length
$\dot{m}$ = mass flow rate
Nu= Nusselt number
P= pressure
Pr = Prandtl number
q''= heat flux
Re = Reynolds number
t= thickness, time
T= temperature
ΔT= wall superheat (T_w -T_{sat})
We = Webber number
X_{tt} = turbulent-turbulent Martinelli factor
x= thermodynamic quality
z = axial direction

Greek Letters

α thermal diffusivity, void fraction
$\Delta\rho = \rho_f - \rho_g$
ε absolute pipe roughness, surface roughness
θ angle of channel with respect to the horizontal, contact angle

θ_c contact angle
μ dynamic viscosity
ν kinematic viscosity
$\nu_{fg} = \nu_g - \nu_f$
ξ percentage error
ρ density
σ surface tension

Subscripts

cr critical
eq equilibrium
f liquid phase
f0 all-liquid
FC forced convection
g vapor phase
g0 all-vapor
H hydraulic
NB nucleate boiling
res resident
s solid phase, surface
sat saturated
tp triple point
w wall

Abbreviations

CHF= critical heat flux
HTC= heat transfer coefficient
ID= inner diameter
LCH4= liquid methane
LH2= liquid hydrogen
LO2= liquid oxygen
LN2= liquid nitrogen
OD= outer diameter
SSD= sample standard deviation

1. Introduction

Liquid hydrogen (LH2), liquid methane (LCH4), and liquid oxygen (LO2) are important cryogenic propellants with broad future applications in space. Transport, storage, and delivery of these and other liquefied cryogens often involve boiling and two-phase flow.

The literature dealing with pool and flow boiling is vast. Monographs and textbooks that present a summary of the well-established models and correlations include [1] and [2]. Most of the existing data and predictive methods are for water and refrigerants, however. The applicability of well-established predictive methods to cryogenic fluids, except for a few correlations for which the databases include cryogens [often liquid nitrogen (LN2)], is at best uncertain.

In two recent articles the authors of this paper reported on comprehensive reviews of the available experimental data dealing with pool [3] and flow boiling [4] of the aforementioned cryogens, where the data were also compared with widely-applied predictive methods for pre-CHF (i.e., nucleate pool boiling, and nucleate boiling and forced convective evaporation in flow boiling) and post-CHF (i.e., pool film boiling, and stable film boiling and dispersed flow boiling during flow boiling). The best performing empirical correlations for pre-CHF and post-CHF boiling regimes were also identified. In this follow-up paper we report on the results of our investigation about the existing experimental data representing critical heat flux for LH2, LCH4, and LO2 in pool and flow boiling.

The objectives of this investigation are thus to:

(1) Compile the existing useful data dealing with pool and flow boiling CHF of LH2, LCH4 and LO2

(2) Assess the applicability or otherwise of well-established CHF correlations for these cryogens

This investigation, as well as [3, 4], only consider pool and flow boiling of the aforementioned cryogens in steady-state experiments. Boiling flow regimes in transient processes, such as chill-down experiments, include transition boiling which is not observed in most steady-state experiments. Hartwig et al. [5] performed a detailed and critical review of available experimental data which included the steady-state flow boiling and critical heat flux of LH2 and LN2. In a separate study Hartwig et al. [6] reviewed the available cryogenic flow boiling data obtained in chill-down (quenching) experiments. For these transient experiments they noted that widely used empirical correlations over predicted the experimental heat transfer data significantly, up to orders of magnitude.

Pool and flow boiling of cryogenic fluids have been studied in the past. The basic boiling regimes and phenomena are known to be common between cryogens and common fluids [7]. However, important differences between cryogenic and common fluids should be expected with respect to details, and deviation between widely-applied boiling heat transfer correlations and experimental data representing cryogenic fluids have been reported [6]. The following are some important differences between common and cryogenic fluids.

- The temperature range for the existence of the liquid phase in cryogenic fluids is small. For example $T_{\mathrm{cr}} - T_{\mathrm{tp}}$ is only about 19 K for LH2 and approximately 100 K for LO2 or LCH4. In comparison, it is about 374 K for water. Wall-fluid temperature differences are thus relatively small in particular in pre-CHF regimes in cryogens.
- The latent heat of vaporization, h_{fg} , is smaller for cryogens in comparison with water, by approximately an order of magnitude. Low h_{fg} impacts all boiling regimes.
- Cryogenic liquids are strongly wetting.

Cryogens act as super hydrophilic on boiling surfaces. Extreme surface wettability (i.e., small contact angle or surface hydrophilicity) leads to smaller bubble departure diameters but higher bubble departure frequency [8], and reduced nucleate boiling heat transfer coefficients. Higher surface wettability increases the critical heat flux as well as the heat transfer coefficient in transition boiling regime [9, 10]. Super hydrophilicity furthermore leads to very high wall superheats for onset of nucleate boiling [11, 12]. Wettability has a significant effect on minimum film boiling as well [9, 13, 14]. When wall temperatures approach the critical temperature, the occurrence of minimum film boiling can in fact be controlled by liquid film superheat [15], rather than hydrodynamic instability as predicted by the hydrodynamic theory of boiling [1].

2. Methodology and Critical Heat Flux Correlations

The open literature has been searched with the purpose of compiling useful experimental data related to boiling of LH2, LCH4 and LO2. The sources of such data can generally be divided into two groups, primary and secondary. Primary sources are publications that directly report on data generated by the authors of a publication or the institution where the experiments have been performed. Secondary sources either depict or report on data generated by others or use such data for model validation or other purposes. Primary sources are evidently more reliable and easier to process, nevertheless secondary sources are also important when dealing with data for which the primary source is difficult to find or even fully understand. The data collected in this study have been reported in a variety of document types, including journal and conference papers as well as reports. Data that are accessible in tabular form are few, and much of the available data are in graphical form. These graphs were digitized and their data extracted. The secondary sources virtually all depict experimental data in graphs where the data are used for model comparison and validation, and occasionally for displaying data trends. The data extracted in this way often need extra calculations and are therefore more prone to uncertainty.

Some of the most widely referenced correlations with respect to the boiling CHF of cryogenic fluids are listed in Table 1 for pool boiling CHF, and in Table 2 for flow boiling CHF. The selected correlations are either of known and proven general applicability or have in the past been applied to cryogens.

Table 1: Correlations for pool boiling CHF

Source	Correlation	Comments
Zuber (1961) [16]	$q''_{\mathrm{CHF}} = \frac{\pi}{24}\sqrt{\rho_{\mathrm{g}}}h_{\mathrm{fg}}(\sigma g \Delta\rho)^{0.25}$ (1)	This correlation is seemingly identical to one derived by Kutateladze [17] where $\frac{\pi}{24}$ is replaced by 0.131.
Lurie and Noyes (1964) [18]	$q''_{\mathrm{CHF}} = 0.144\sqrt{\rho_{\mathrm{g}}}h_{\mathrm{fg}}(\sigma g \Delta\rho)^{0.25} Pr_{\mathrm{f}}^{-0.245}\left(\frac{\rho_{\mathrm{f}}-\rho_{\mathrm{g}}}{\rho_{\mathrm{f}}}\right)^{0.25}$ (2)	
Sun and Lienhard (1970) [19]	$q''_{\mathrm{CHF}} = 0.149\sqrt{\rho_{\mathrm{g}}}h_{\mathrm{fg}}(\sigma g \Delta\rho)^{0.25}$ (3)	
Kandlikar (2001) [20]	$q''_{\mathrm{CHF}} = \left(\frac{1+cos\theta_{\mathrm{c}}}{16}\right)\left[\frac{2}{\pi}+\frac{\pi}{4}(1+cos\theta_{\mathrm{c}})cos\theta\right]^{0.5}\sqrt{\rho_{\mathrm{g}}}h_{\mathrm{fg}}(\sigma g \Delta\rho)^{0.25}$ (4)	

Table 2: Correlations for flow boiling CHF

Source	Correlation	Comments
Von Glaun and Lewis (1960) [21]	$f(X) = \frac{q''_{CHF} A_s}{\dot{m}[(h_{f,sat} - h_f) + h_{fg}]} \left(\frac{L}{D_H}\right)^{0.135} \left(\frac{T_{sat}}{T_f}\right)^{0.4}$ (5) $f(G) = Re_{g0} Pr_g^{0.4} \left(\frac{\mu_f^2}{D_H \sigma \rho_g}\right)^{0.19} \left(\frac{T_{sat}}{T_f}\right)^{0.4} \left(\frac{L}{D_H}\right)^{-1.67}$ (6) $f(X) = 7.8947 f(G)^{-0.483}$ (7)	The original correlation was presented graphically. Eq. 7 is the result of a power regression digitized using PlotDigitizer. Developed from water and cryogenic data
Katto and Ohno (1984) [22]	$q''_{CHF} = q''_{Co}\left[1 + \frac{K(h_{f,sat} - h_f)}{h_{fg}}\right]$ (8) $q''_{Co,2} = C_{Ko}\left(\frac{\sigma \rho_f}{G^2 L}\right)^{0.043} \frac{D_H}{L} G h_{fg}$ (9) $q''_{Co,3} = 0.1\left(\frac{\rho_g}{\rho_f}\right)^{0.133}\left(\frac{\sigma \rho_f}{G^2 L}\right)^{0.333} \frac{G h_{fg}}{1 + 0.0031\frac{L}{D_H}}$ (10) $q''_{Co,4} = 0.098\left(\frac{\rho_g}{\rho_f}\right)^{0.133}\left(\frac{\sigma \rho_f}{G^2 L}\right)^{0.433} \frac{\left(\frac{L}{D_H}\right)^{0.27}}{1 + 0.0031\frac{L}{D_H}} G h_{fg}$ (11) $q''_{Co,5} = 0.0384\left(\frac{\rho_g}{\rho_f}\right)^{0.6}\left(\frac{\sigma \rho_f}{G^2 L}\right)^{0.173} \frac{G h_{fg}}{1 + 0.28\left(\frac{\sigma \rho_f}{G^2 L}\right)^{0.233}\frac{L}{D_H}}$ (12) $q''_{Co,13} = 0.234\left(\frac{\rho_g}{\rho_f}\right)^{0.513}\left(\frac{\sigma \rho_f}{G^2 L}\right)^{0.433} \frac{\left(\frac{L}{D_H}\right)^{0.27}}{1 + 0.0031\frac{L}{D_H}} G h_{fg}$ (13) $K_6 = \frac{1.043}{4 C_{Ko}\left(\frac{\sigma \rho_f}{G^2 L}\right)^{0.043}}$ (14) $K_7 = \frac{5}{6}\left[\frac{0.0124 + \frac{D_H}{L}}{\left(\frac{\rho_g}{\rho_f}\right)^{0.133}\left(\frac{\sigma \rho_f}{G^2 L}\right)^{0.333}}\right]$ (15)	The numerical values in the subscripts are consistent with the equation numbers in the source material. Developed from R-12 data.

	$K_9 = 1.12\left[\frac{1.52\left(\frac{\sigma\rho_{\mathrm{f}}}{G^2L}\right)^{0.233}+\frac{D_{\mathrm{H}}}{L}}{\left(\frac{\rho_{\mathrm{g}}}{\rho_{\mathrm{f}}}\right)^{0.6}\left(\frac{\sigma\rho_{\mathrm{f}}}{G^2L}\right)^{0.173}}\right]$ (16) $q''_{Co} = \begin{cases} \min\left(q''_{Co,2}, q''_{Co,3}, q''_{Co,3}\right), & \frac{\rho_{\mathrm{g}}}{\rho_{\mathrm{f}}} < 0.15 \\ \min\left(q''_{Co,2}, q''_{Co,5}, q''_{Co,13}\right), & \frac{\rho_{\mathrm{g}}}{\rho_{\mathrm{f}}} > 0.15 \end{cases}$ (17) $K = \begin{cases} \max(K_6, K_7), & \frac{\rho_{\mathrm{g}}}{\rho_{\mathrm{f}}} < 0.15 \\ \max(K_6, K_7, K_9), & \frac{\rho_{\mathrm{g}}}{\rho_{\mathrm{f}}} > 0.15 \end{cases}$ (18)	

Table 2 continued.

Source	Correlation	Comments
Shah (1987) [23], applied in [1]	For the UCC version: $Bo = \frac{q''_{CHF}}{Gh_{fg}} = 0.124\left(\frac{D_H}{L_E}\right)^{0.89}\left(\frac{10^4}{Y}\right)^n (1 - x_{iE})$ (19) $L_E = \begin{cases} L, & x_{in} \le 0 \\ L + \frac{D_H x_{in}}{4Bo}, & x_{in} > 0 \end{cases}$ (20) $x_{iE} = \begin{cases} x_{in}, & x_{in} \le 0 \\ 0, & x_{in} > 0 \end{cases}$ (21) $Y = \frac{GD_H C_{p,f}}{k_f}\left(\frac{\rho_f^2 g D_H}{G^2}\right)^{-0.4}\left(\frac{\mu_f}{\mu_g}\right)^{0.6}$ (22) For the fluids considered in this work, $n = \begin{cases} 0, & Y \le 10^4 \\ \left(\frac{D_H}{L_E}\right)^{0.54}, & 10^4 < Y \le 10^6 \\ \frac{0.12}{\sqrt{1-x_{iE}}}, & Y > 10^6 \end{cases}$ (23) For the LCC version: $Bo = \frac{q''_{CHF}}{Gh_{fg}} = F_E F_x Bo_0$ (24) $F_E = 1.54 - 0.032\left(\frac{L}{D_H}\right)$ (25) F_E is required to have a maximum value of unity if the above equation exceeds unity. $Bo_0 = \max(Bo_{01}, Bo_{02}, Bo_{03})$ (26) where $Bo_{01} = 15Y^{-0.612}$ (27) $Bo_{02} = 0.082Y^{-0.3}\left[1 + 1.45\left(\frac{P}{P_{cr}}\right)^{4.03}\right]$ (28) $Bo_{03} = 0.0024Y^{-0.105}\left[1 + 1.15\left(\frac{P}{P_{cr}}\right)^{3.39}\right]$ (29) If $x_{eq} \ge 0$ then $F_x = F_3\left[1 + \frac{(F_3^{-0.29} - 1)\left(\frac{P}{P_{cr}} - 0.6\right)}{0.35}\right]^c$ (30)	Shah recommends using the UCC method when $Y \le 10^6$ or $L_E > \frac{160}{\left(\frac{P}{P_{cr}}\right)^{1.14}}$; otherwise the version yielding the lower *Bo* should be used. This correlation is based on a vast amount of data and can be applied to various fluids

	$F_3 = \left(\frac{1.25\times10^5}{Y}\right)^{0.833x_{\mathrm{eq}}}$ (31) $c = \begin{cases} 0, & \frac{P}{P_{\mathrm{cr}}} \le 0.6 \\ 1, & \frac{P}{P_{\mathrm{cr}}} > 0.6 \end{cases}$ (32) If $x_{\mathrm{eq}} < 0$ then $F_{\mathrm{x}} = F_1\left[1 - \frac{(1-F_2)\left(\frac{P}{P_{\mathrm{cr}}}-0.6\right)}{0.35}\right]^b$ (33) $F_1 = 1 + 0.0052(-x_{\mathrm{eq}})^{0.88}Y^{0.41}$ (34) Y is required to have a maximum value of 1.4×10^7 if Eq. 180 exceeds 1.4×10^7. $F_2 = \begin{cases} F_1^{-0.42}, & F_1 \le 4 \\ 0.55, & F_1 > 4 \end{cases}$ (35) $b = \begin{cases} 0, & \frac{P}{P_{\mathrm{cr}}} \le 0.6 \\ 1, & \frac{P}{P_{\mathrm{cr}}} > 0.6 \end{cases}$ (36)	
Mudawar and Maddox (1990), applied in [5]	$q''_{CHF} = 0.161Gh_{\mathrm{fg}}\left(\frac{\rho_{\mathrm{g}}}{\rho_{\mathrm{f}}}\right)^{15/23} We_{\mathrm{f0}}^{-8/23}\left(\frac{L}{D_{\mathrm{H}}}\right)^{1/23}$ (37) $We_{\mathrm{f0}} = \frac{G^2L}{\rho_{\mathrm{f}}\sigma}$ (38)	Developed using FC-72 data through a rectangular channel

Table 2 continued.

Source	Correlation	Comments
Katto (1992), applied in [1]	$q''_{\mathrm{b}} \geq \frac{\rho_{\mathrm{f}}\delta_{\mathrm{film}}h_{\mathrm{fg}}}{t_{\mathrm{res}}}$ (39) where $\delta_{\mathrm{film}} = 1.705\times10^{-3}\pi\left(\frac{\rho_{\mathrm{g}}}{\rho_{\mathrm{f}}}\right)^{0.4}\left(1+\frac{\rho_{\mathrm{g}}}{\rho_{\mathrm{f}}}\right)\frac{\sigma}{\rho_{\mathrm{g}}}\left(\frac{\rho_{\mathrm{g}}h_{\mathrm{fg}}}{q''_{\mathrm{b}}}\right)^{2}$ (40) $q''_{\mathrm{b}} = q''_{\mathrm{w}} - h_{\mathrm{FC}}\left(T_{\mathrm{w}} - \overline{T_{\mathrm{f}}}\right)$ (41) where h_{FC} is the heat transfer coefficient of Dittus and Boelter (1985) [24] $t_{\mathrm{res}} = \frac{2\pi\sigma(\rho_{\mathrm{f}}+\rho_{\mathrm{g}})}{\rho_{\mathrm{f}}\rho_{\mathrm{g}}(U_{\mathrm{B}}-U_{\mathrm{fB}})^{3}}$ (42) $U_{\mathrm{B}} - U_{\mathrm{fB}} = KU_{\mathrm{f},\delta}$ (43) where $U_{\mathrm{f},\delta}$ is the turbulent boundary layer velocity found from the universal boundary layer velocity profile, and K is found as outlined below: $K_{\mathrm{a}} = \frac{242[1+K_1(0.355-\alpha)][1+K_2(0.1-\alpha)]}{\left[0.0197+\left(\frac{\rho_{\mathrm{g}}}{\rho_{\mathrm{f}}}\right)^{0.733}\right]\left[1+90.3\left(\frac{\rho_{\mathrm{g}}}{\rho_{\mathrm{f}}}\right)^{3.68}\right]}Re^{-0.8}$ (44) $K_{\mathrm{b}} = \frac{22.4[1+K_3(0.355-\alpha)]}{\left(\frac{\rho_{\mathrm{g}}}{\rho_{\mathrm{f}}}\right)^{1.28}}Re^{-0.8}$ (45) $K_1 = \begin{cases} 0, & \alpha > 0.355 \\ 3.76, & \alpha < 0.355 \end{cases}$ (46)	Its range is limited to void fractions below 70%

	$K_2 = \begin{cases} 0, & \alpha > 0.1 \\ 2.62, & \alpha < 0.1 \end{cases}$ (47) $K_3 = \begin{cases} 0, & \alpha > 0.355 \\ 1.33, & \alpha < 0.355 \end{cases}$ (48) The following $\left(\frac{\rho_g}{\rho_f}\right)_b$ threshold is obtained by intersecting Eqs. 44 and 45. K is then determined by $K = \begin{cases} K_a, & \left(\frac{\rho_g}{\rho_f}\right) > \left(\frac{\rho_g}{\rho_f}\right)_b \\ K_b, & \left(\frac{\rho_g}{\rho_f}\right) < \left(\frac{\rho_g}{\rho_f}\right)_b \end{cases}$ (49)	

Table 2 continued.

Hall and Mudawar (2000), applied in [5]	$q''_{\mathrm{CHF}} = \frac{0.0722 We_{D_{\mathrm{H}}}^{-0.312} \left(\frac{\rho_{\mathrm{f}}}{\rho_{\mathrm{g}}}\right)^{-0.644} \left[1 - 0.9 \left(\frac{\rho_{\mathrm{f}}}{\rho_{\mathrm{g}}}\right)^{0.724} x_{\mathrm{in}}\right]}{1 + 0.2599 We_{D_{\mathrm{H}}}^{-0.312} \left(\frac{\rho_{\mathrm{f}}}{\rho_{\mathrm{g}}}\right)^{0.08} \left(\frac{L}{D_{\mathrm{H}}}\right)} G h_{\mathrm{fg}}$ (50) $We_{D_{\mathrm{H}}} = \frac{G^2 D_{\mathrm{H}}}{\rho_{\mathrm{f}} \sigma}$ (51)	Developed using 5544 water data points

Application of most flow boiling correlations requires knowledge of the local quality, sometimes not provided by the authors of experimental data. In these cases, the quality at the measurement location was calculated by solving the following one-dimensional momentum and energy conservation equations, respectively, assuming homogenous equilibrium mixture (HEM) flow [1]:

$$\frac{\mathrm{d}x}{\mathrm{d}z} = \frac{-Gg\sin\theta + \frac{4q''_{\mathrm{w}}}{D_{\mathrm{H}}}}{Gh_{\mathrm{fg}} + G^3(v_{\mathrm{f}} + xv_{\mathrm{fg}})v_{\mathrm{fg}}} \quad (52)$$

$$\frac{\mathrm{d}P}{\mathrm{d}z} = \frac{-g\sin\theta}{(v_{\mathrm{f}} + xv_{\mathrm{fg}})} - \frac{f_{\mathrm{TP}}}{D_{\mathrm{H}}}\frac{G^2}{2}\left(v_{\mathrm{f}} + xv_{\mathrm{fg}}\right) - G^2 v_{\mathrm{fg}}\frac{\mathrm{d}x}{\mathrm{d}z} \quad (53)$$

The two-phase friction factor is determined using the correlation of Beattie and Whalley, [25], whereby,

$$\frac{1}{\sqrt{4f_{\mathrm{TP}}}} = 1.14 - 2\log_{10}\left(\frac{\varepsilon}{D_{\mathrm{H}}} + \frac{9.35}{Re_{\mathrm{TP}}\sqrt{4f_{\mathrm{TP}}}}\right) \quad (54)$$

$$Re_{\mathrm{TP}} = \frac{GD_{\mathrm{H}}}{\mu_{\mathrm{TP}}} \quad (55)$$

$$\mu_{\mathrm{TP}} = \alpha\mu_{\mathrm{g}} + \mu_{\mathrm{f}}(1-\alpha)(1+2.5\alpha) \quad (56)$$

$$\rho_{\mathrm{TP}} = \left(\frac{x}{\rho_{\mathrm{g}}} + \frac{1-x}{\rho_{\mathrm{f}}}\right)^{-1} \quad (57)$$

$$\alpha = \left[1 + \left(\frac{1-x}{x}\right)\frac{\rho_{\mathrm{g}}}{\rho_{\mathrm{f}}}\right]^{-1} \quad (58)$$

The percentage error for every data point is calculated from

$$\xi = \frac{q''_{\mathrm{predicted}} - q''_{\mathrm{exp}}}{q''_{\mathrm{exp}}} \times 100 \quad (59)$$

Evidently, values of the percentage error closer to zero indicate better agreement. The mean and sample standard deviation of these percentage errors are computed respectively by

$$\bar{\xi} = \frac{\sum_i^N \xi_i}{N} \quad (60)$$

$$\xi_{SSD} = \sqrt{\frac{\sum_i^N (\xi - \bar{\xi})^2}{N-1}} \quad (61)$$

Two other metrics are the percentage of predicted heat fluxes that are within 30% and 100% of the experimental data. The mathematical formulations that determined whether a data point falls within the aforementioned bounds are

$$\xi_{30} = \begin{cases} \text{success}, & -0.23 \le \xi \le 0.3 \\ \text{failure}, & \text{otherwise} \end{cases} \quad (62)$$

$$\xi_{100} = \begin{cases} \text{success}, & -0.5 \leq \xi \leq 1.0 \\ \text{failure}, & \text{otherwise} \end{cases} \quad (63)$$

More detailed information can be found in [26].

Table 3: Summary of past studied for the pool boiling CHF

Source	Data Type	Boiling Regime	Geometry & Orientation	Material	Operating Condition	Additional Comments
Mulford and Nigon [27]	Plots	Pool nucleate Pool film	Cylinder (horizontal) D= 12 mm	Copper	Atmospheric pressure	Fluids: LH2, LN2 Cannot access paper; data extracted from Seader et al. [28] Roughness unspecified
Graham et al. [29]	Plots	Pool nucleate Pool film	Rectangular plate (vertical) Dimensions not specified but estimated to be: L= 33.53 cm W= 10.36 cm	Chromel-A heating element on a Bakelite block	Gravity= 1g-10 g $\Delta T_{sub} \leq 2.77$ K For nucleate: P= 2.9 bar, 3.4 bar , 3.6 bar, 6.3 bar, 6.7 bar For film: P= 3.5 bar, 6.7 bar	Fluids: LH2 Roughness unspecified
Merte [30]	Plots	Pool nucleate Pool film MFB	Sphere D= 2.54 cm Square plate (horizontal, vertical) L= 2.54 cm Wire D= 0.1346 mm	Copper (sphere, plate) Fiberglass (plate) Platinum (wire)	Gravity≤1g P= 1 bar, 1.6 bar, 2.6 bar	Fluids: LH2, LN2 Roughness unspecified
Ohira and Furumoto [31]	Plots	Pool nucleate	Disk (horizontal, vertical) D= 25 mm	Copper	P= 0.07 bar, 1.013 bar	Fluids: Slush H2, LH2, LN2, slush N2 $\varepsilon = 1\ \mu m$
Ohira [32]	Plots	Pool nucleate CHF	Disk (horizontal, vertical) D= 25 mm	Copper	P= 0.07 bar, 1.013 bar	Fluids: LH2, LN2 Compared with correlations: For nucleate: Rohsenow (1952), Clark (1975) For CHF: Kutateladze (1959) Identical data as in source [31]

Shirai et al. [33]	Plots	Pool nucleate CHF	Rectangular plate (horizontal) L= 10 mm W= 100 mm	Manganin	P= 1.1 bar, 2 bar, 3 bar, 7 bar, 7.2 bar $\Delta T_{sub} \leq 10$ K	Fluids: LH_2 Compared with correlations: Kutateladze (1952), Rohsenow (1952), Labountsov (1972) Roughness unspecified
Sciance et al.[34]	Plots	Pool nucleate Pool film CHF MFB	Cylinder (horizontal) D= 2.06 cm	Gold	P= 1 bar, 2.3 bar, 4.6 bar, 6.9 bar, 9.2 bar, 13.8 bar, 18.4 bar, 23 bar, 27.6 bar, 32.2 bar, 36.8 bar, 41.4 bar	Fluids: LCH_4 Compared with correlations: For nucleate: Rohsenow (1952), Forster and Greif (1958), Madejski (1965) For CHF: Lurie and Noyes (1963-1964) For MFB: Berenson (1961) New film boiling correlation proposed Roughness unspecified
Kosky and Lyon [35]	Plots	Pool nucleate	Disk (horizontal) D= 1.9 cm	Platinum	P= 0.25 bar, 0.55 bar, 2.2 bar, 4.3 bar, 8.2 bar, 16.7 bar, 25.2 bar, 32.9 bar, 42.8 bar, 49 bar	Fluids: LCH_4, LO_2, LN_2, LAr, CF_4 Compared with correlations: Rohsenow (1952), Forster-Zuber (1954), Forster-Greif (1958), Gilmour (1958), McNelly (1953), Kutateladze (1952), Borishanskiy-Minchenko (1961) Roughness unspecified
Lyon et al. [36]	Plots, Tables	Pool nucleate	Ring (horizontal) OD= 6.86 cm ID= 6.45 cm	Platinum	P= 1 bar, 2 bar, 4.1 bar, 8 bar, 15.7 bar, 21.1 bar, 26 bar, 32.5 bar, 41.3 bar	Fluids: LO_2, LN_2 Compared with correlations: Rohsenow (1952), Kutateladze (1952) Roughness unspecified

3. POOL BOILING

Table 3 is a summary of the past studies dealing with pool boiling CHF of LH2. As noted, useful data are available only from five independent sources. Few CHF experiments for LH2 could be found, but some of the nucleate boiling experiments provided heat flux vs. wall superheat data up to the point of burnout. In these experiments, the surface underwent heating and therefore followed the boiling curve from left to right, i.e., in the direction of increasing wall superheat. The burnout point corresponds to the CHF and was determined as the point beyond which the heat flux no longer showed the expected dependence on wall superheat that is characteristic of nucleate boiling. This approach may be interpreted and justified as representing a lower estimate of CHF.

Table 4 shows the statistical results from the four correlations used to predict the pool boiling CHF, and the individual correlation comparisons can be seen in Figures 1 through 4. Table 4 does not include the data of Roubeau [37], as all correlations over predicted the data by at least an order of magnitude in all cases. Additionally, two points from Merte [30] conducted on Fiberglass as the heated surface were eliminated. All four tested correlations are of similar formulation and can predict the CHF within a factor of two for more than 80% of the data.

Based on the 25 data points taken from five independent sources, it is suggested that the correlation of Sun and Lienhard [19] (Eq. 3) be used to predict the pool CHF of LH2. It performs the best statistically and can predict the CHF within a factor of two 90% of the time. It should be noted, however, that the number of available data suitable for analysis is hardly enough to effectively distinguish the nuances among these correlations.

Table 4: Mean and standard deviation of ξ, and percentage of experimental data points that fall within a factor of 2.0 and 1.3 of correlations for the pool CHF of LH2

	Zuber [16]	Sun and Lienhard [19]	Lurie and Noyes [18]	Kandlikar [20]
Mean	-0.13	-0.01	-0.14	0.01
Standard deviation	0.25	0.28	0.25	0.44
Percentage of data for which $-0.5 \le \xi \le 1.0$	83.33	91.67	83.33	83.33
Percentage of data for which $-0.23 \le \xi \le 0.3$	75.00	75.00	70.83	33.33

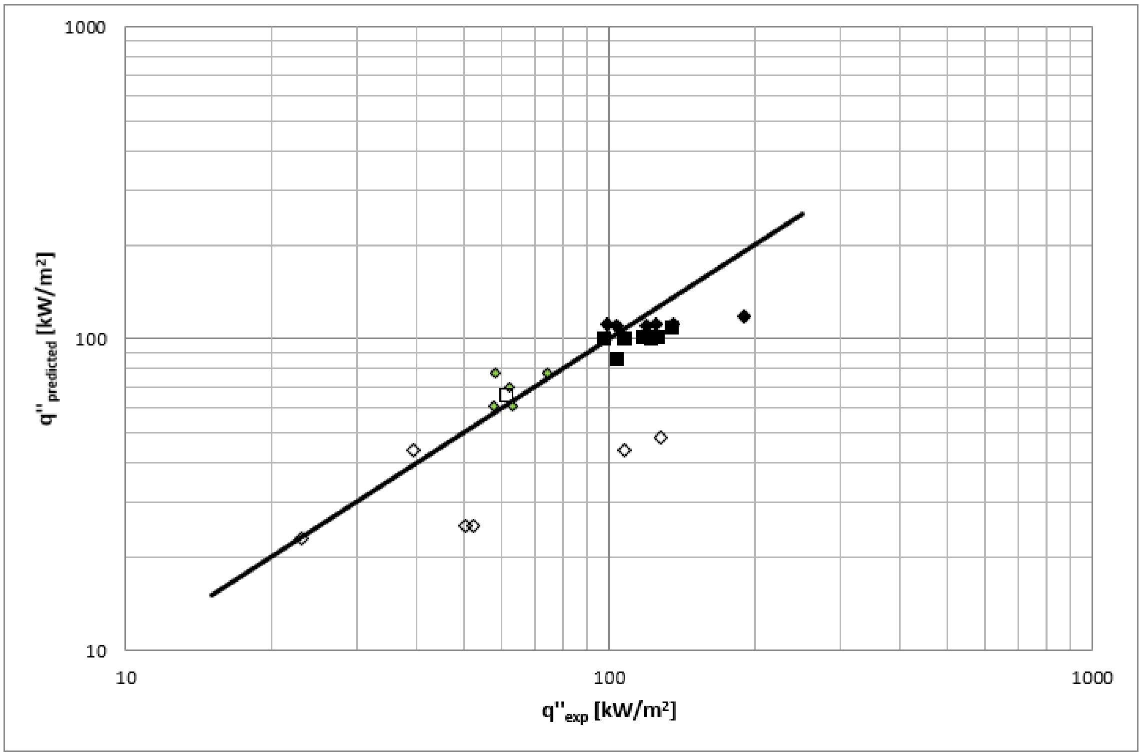

Figure 1: Comparison between LH2 pool burnout points and the CHF correlation of Zuber [16]. The solid line is the identity line.

◆ Graham et al. ◆ Merte ◇ Ohira and Furumoto ■ Shirai et al. □ Mulford and Nigon

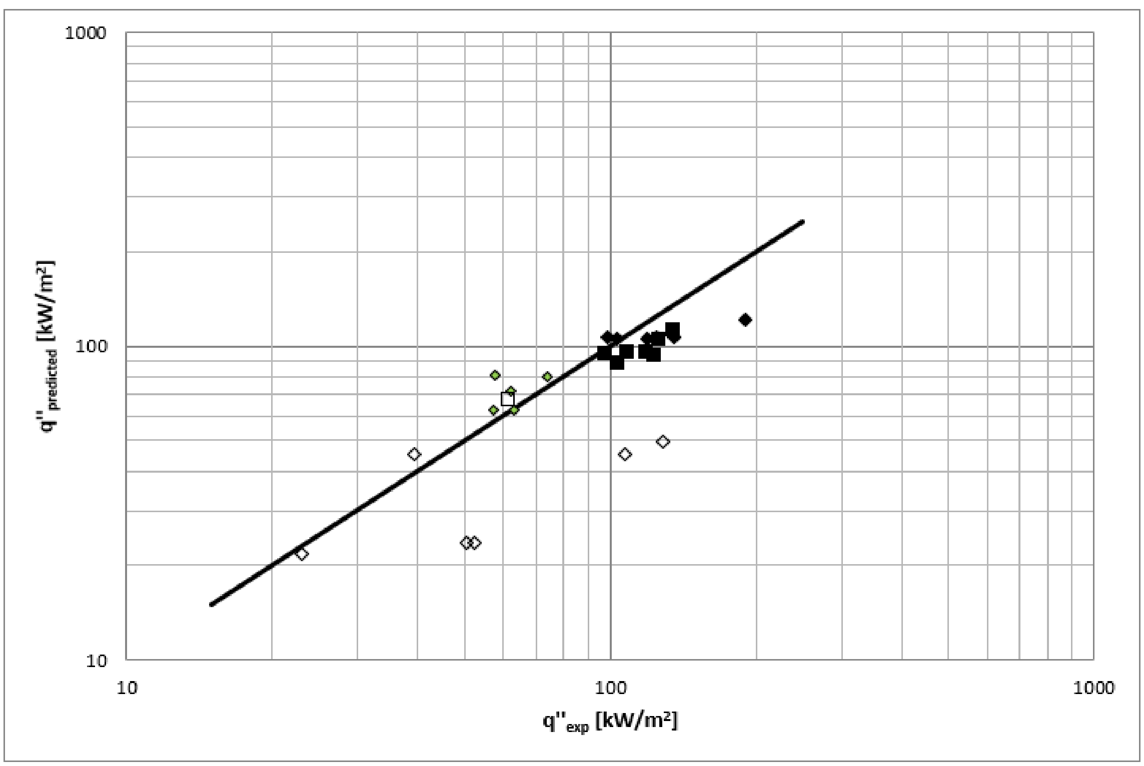

Figure 2: Comparison between LH2 pool burnout points and the CHF correlation of Lurie and Noyes [18]. The solid line is the identity line.

◆ Graham et al. ◆ Merte ◇ Ohira and Furumoto ■ Shirai et al. □ Mulford and Nigon

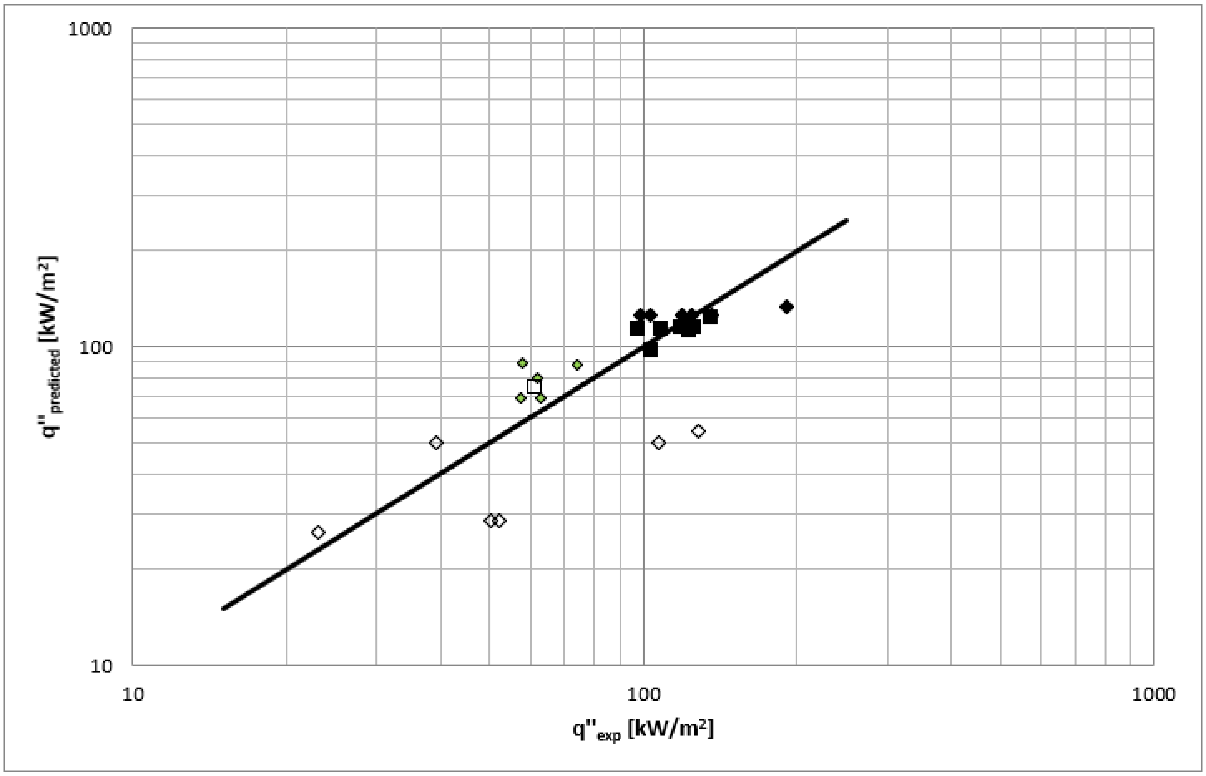

Figure 3: Comparison between LH2 pool burnout points and the CHF correlation of Sun and Lienhard [19]. The solid line is the identity line.

◆ Graham et al. ◆ Merte ◇ Ohira and Furumoto ■ Shirai et al. □ Mulford and Nigon

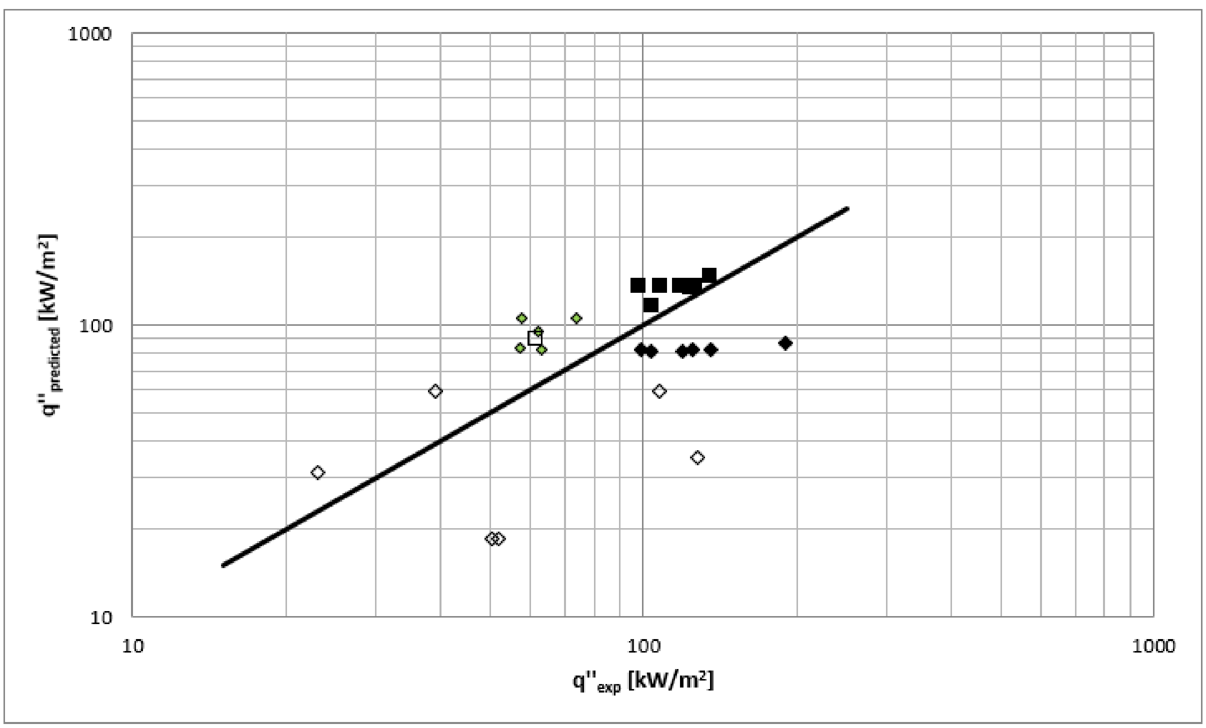

Figure 4: Comparison between LH2 pool burnout points and the CHF correlation of Kandlikar [20]. The solid line is the identity line.

◆ Graham et al. ◆ Merte ◇ Ohira and Furumoto ■ Shirai et al. □ Mulford and Nigon

Only two experiments with useful CHF data for the pool boiling of LCH4 could be found, as noted in Table 3. In both cases, the burnout point was extracted from the boiling curve results in the manner described earlier. Table 5 shows the statistical results from the four correlations used to predict the pool boiling CHF, and the individual correlation comparisons can be seen in Figures 5-8. All four tested correlations are of similar formulation and can predict the CHF within a factor two more than 70% of the time, although a severe scarcity of data exists. Based on the 15 data points taken from the two available sources, it is suggested that the correlation of Lurie and Noyes [18] (Eq. 2) be used to estimate the pool CHF of LCH4. Of the considered correlations, it performs the best statistically and predicts the CHF of the available data within a factor of two over 90% of the time.

Table 5: Mean and standard deviation of ξ, and percentage of experimental data points that fall within a factor of 2.0 and 1.3 of correlations for the pool CHF of LCH4

	Zuber [16]	Sun and Lienhard [19]	Lurie and Noyes [18]	Kandlikar [20]
Mean	0.17	0.33	-0.05	0.60
Standard deviation	0.41	0.47	0.34	0.56
Percentage of data for which $-0.5 \leq \xi \leq 1.0$	86.67	86.67	93.33	73.33
Percentage of data for which $-0.23 \leq \xi \leq 0.3$	60.00	53.33	73.33	13.33

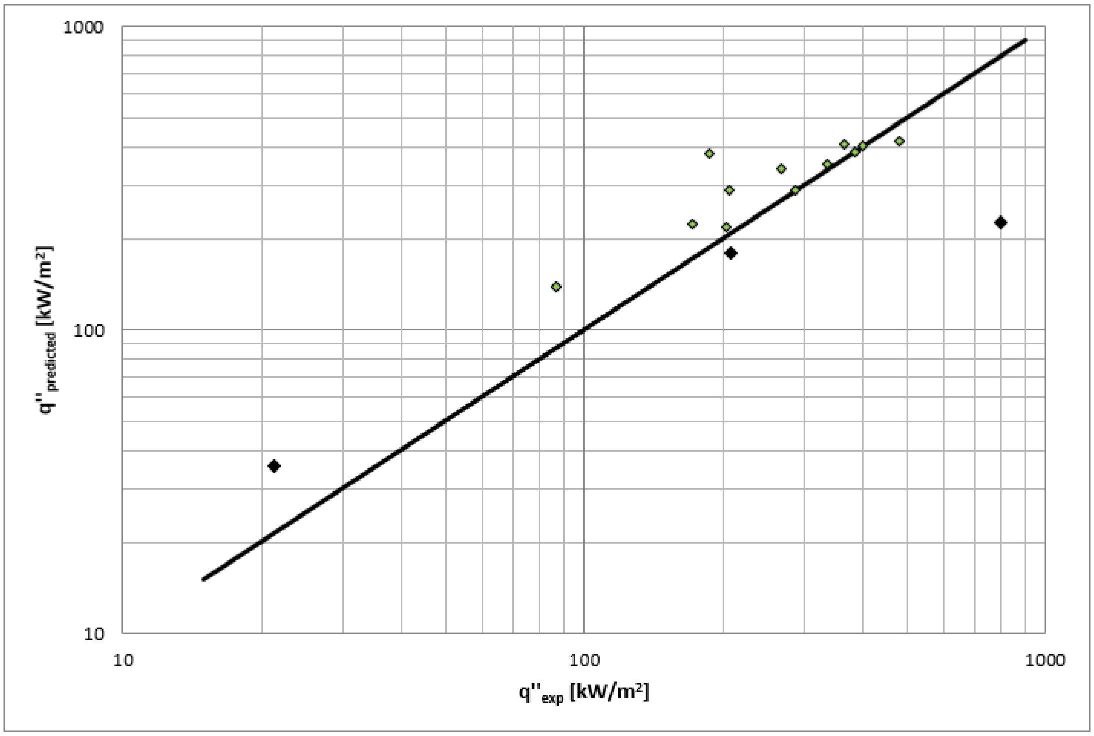

Figure 5: Comparison between LCH4 pool burnout points and the CHF correlation of Zuber [16]. The solid line is the identity line.

◆ Kosky and Lyon ◇ Sciance et al.

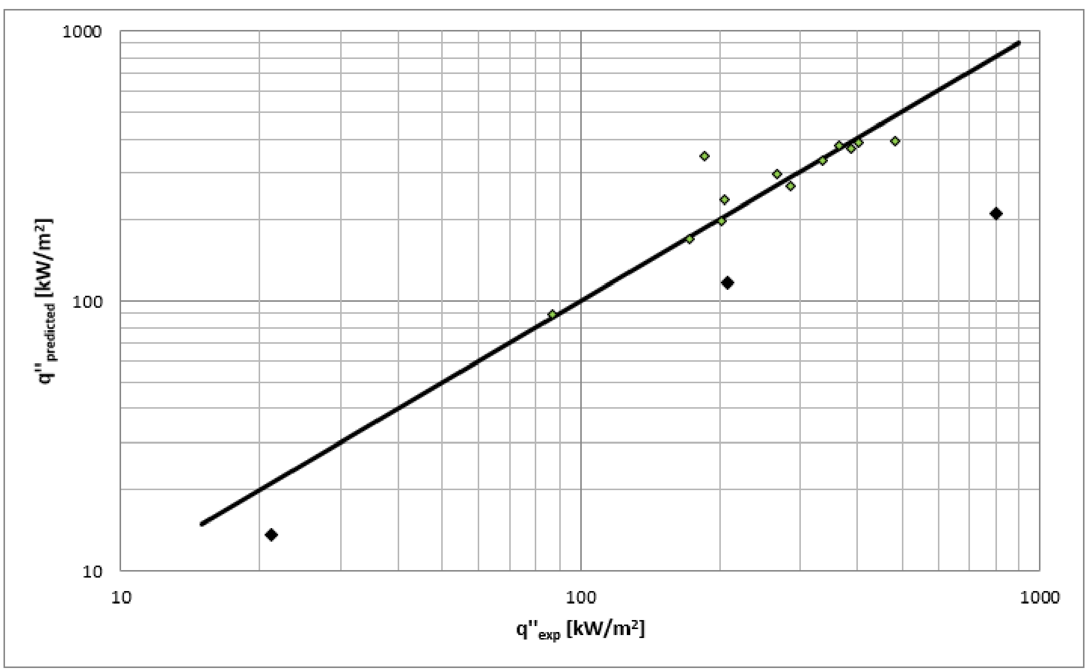

Figure 6: Comparison between LCH4 pool burnout points and the CHF correlation of Lurie and Noyes [18]. The solid line is the identity line.

◆ Kosky and Lyon ◇ Sciance et al.

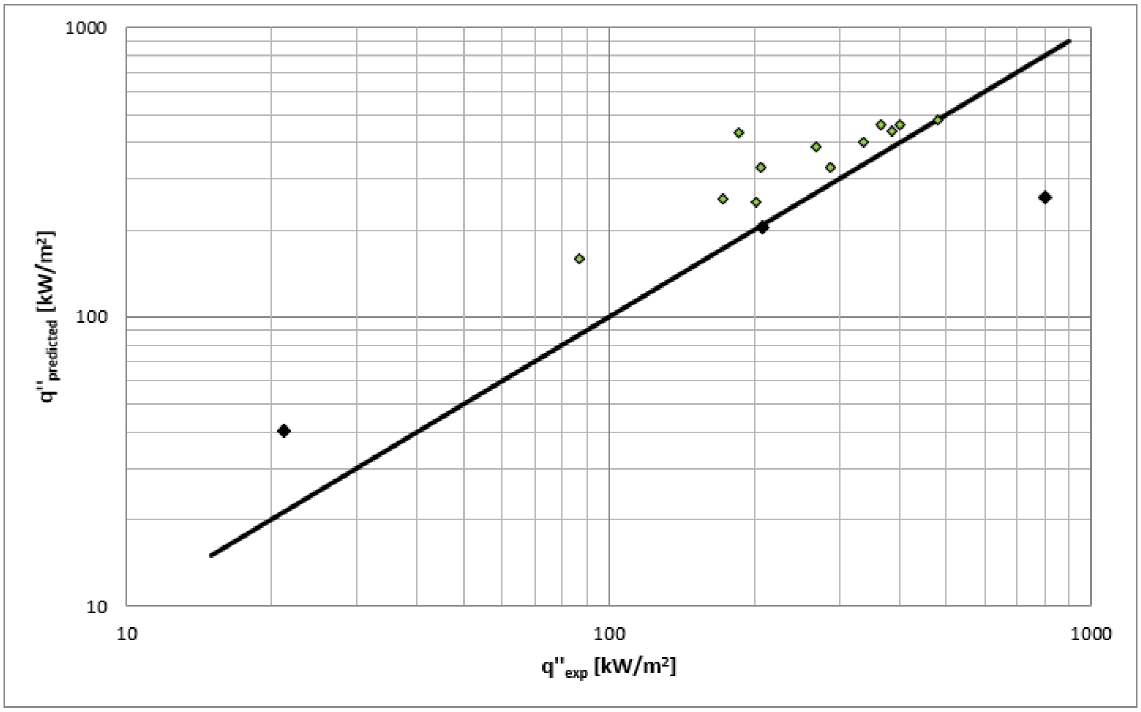

Figure 7: Comparison between LCH4 pool burnout points and the CHF correlation of Sun and Lienhard [19]. The solid line is the identity line.

◆ Kosky and Lyon ◇ Sciance et al.

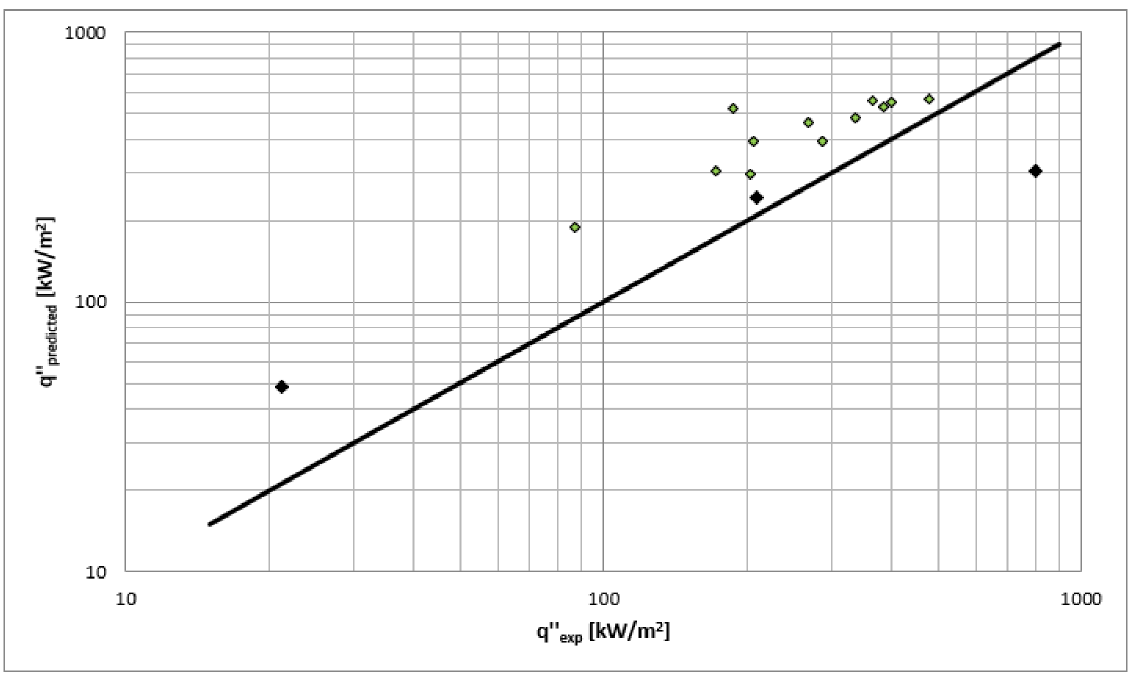

Figure 8: Comparison between LCH4 pool burnout points and the CHF correlation of Kandlikar [20]. The solid line is the identity line.

◆ Kosky and Lyon ◇ Sciance et al.

Only two experiments with useful CHF data for the pool boiling of LO2 could be found. In both cases, the burnout point was indicated on figures displaying heat flux vs. superheat data. Table 6 shows the statistical results from the four correlations used to predict the pool boiling CHF, and the individual correlation comparisons can be seen in Figures 9 through 12. All four tested correlations are of similar formulation and can predict the CHF within a factor two about 70% of the time, although a severe lack of data exists. Based on the 19 data points taken from the two available sources, it is suggested that the correlation of Sun and Lienhard [19] (Eq. 3) be used to predict the pool CHF of LO2. The data taken from Kosky and Lyon [35] is consistently under predicted by all the correlations considered, particularly at larger superheats, while the data of Lyon et al. [36] is in better agreement with the correlations. The correlation of Sun and Lienhard predicts the available CHF data to within a factor of two about 74% of the time.

Table 6: Mean and standard deviation of ξ, and percentage of experimental data points that fall within a factor of 2.0 and 1.3 of correlations for the pool CHF of LO2

	Zuber [16]	Sun and Lienhard [19]	Lurie and Noyes [18]	Kandlikar [20]
Mean	-0.24	-0.14	-0.38	0.03
Standard deviation	0.42	0.48	0.24	0.57
Percentage of data for which $-0.5 \leq \xi \leq 1.0$	73.68	73.68	68.42	78.95
Percentage of data for which $-0.23 \leq \xi \leq 0.3$	47.37	63.16	36.84	52.63

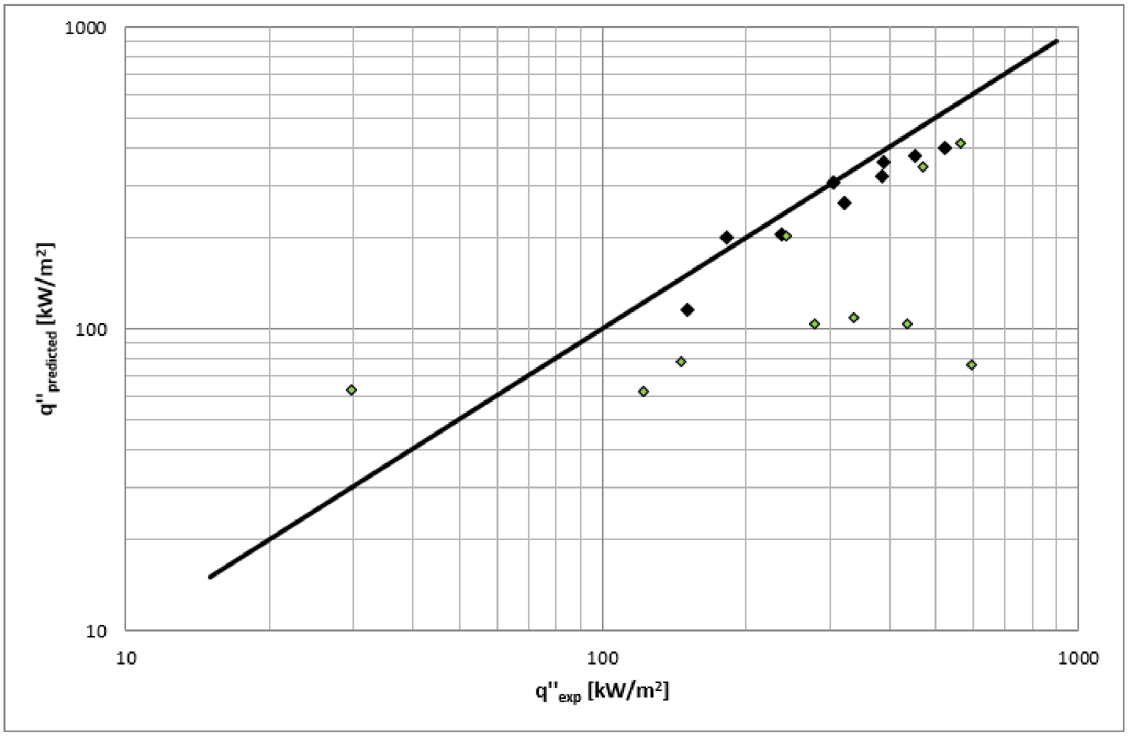

Figure 9: Comparison between LO2 pool burnout points and the CHF correlation of Zuber [16]. The solid line is the identity line.

◆ Lyon et al. ◇ Kosky and Lyon

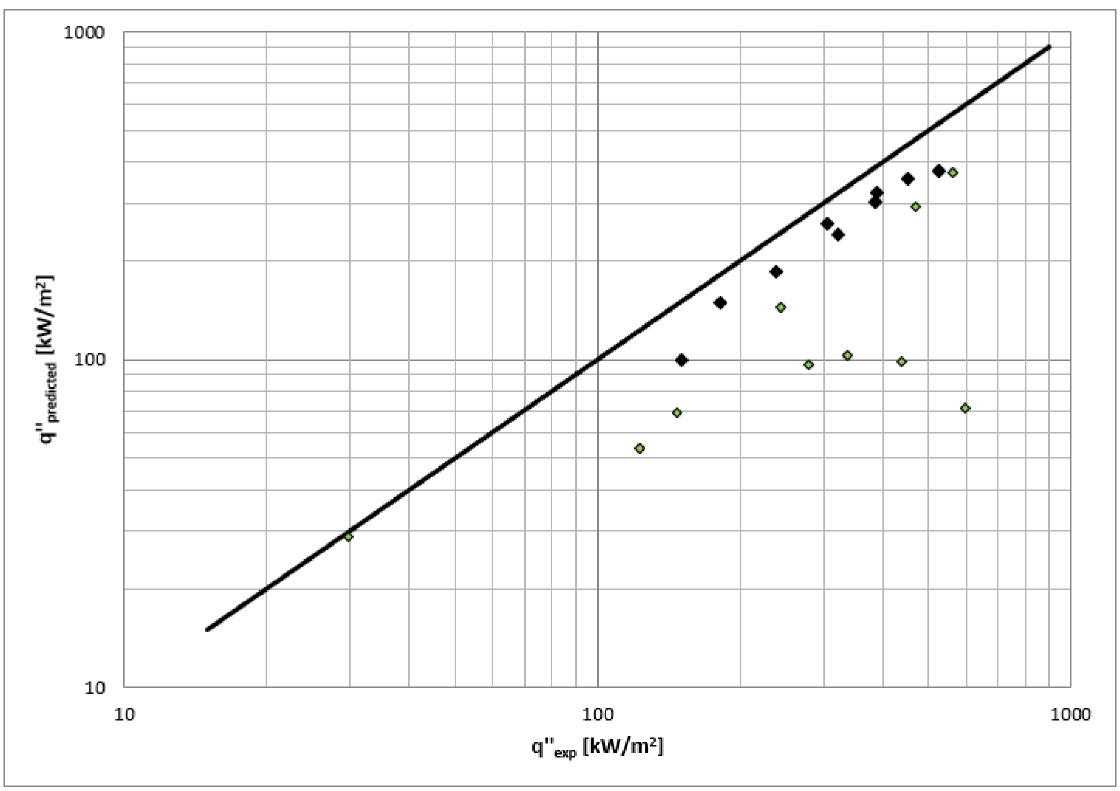

Figure 10: Comparison between LO2 pool burnout points and the CHF correlation of Lurie and Noyes [18]. The solid line is the identity line.

◆ Lyon et al. ◇ Kosky and Lyon

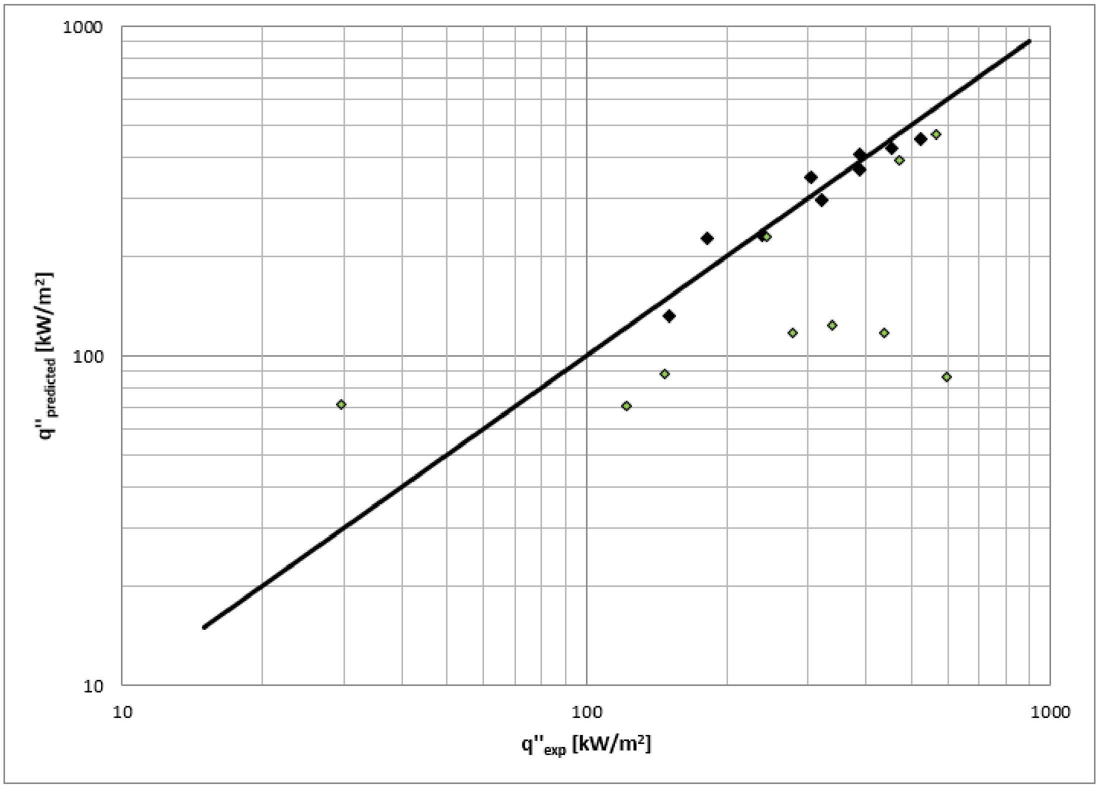

Figure 11: Comparison between LO2 pool burnout points and the CHF correlation of Sun and Lienhard [19]. The solid line is the identity line.

◆ Lyon et al. ◆ Kosky and Lyon

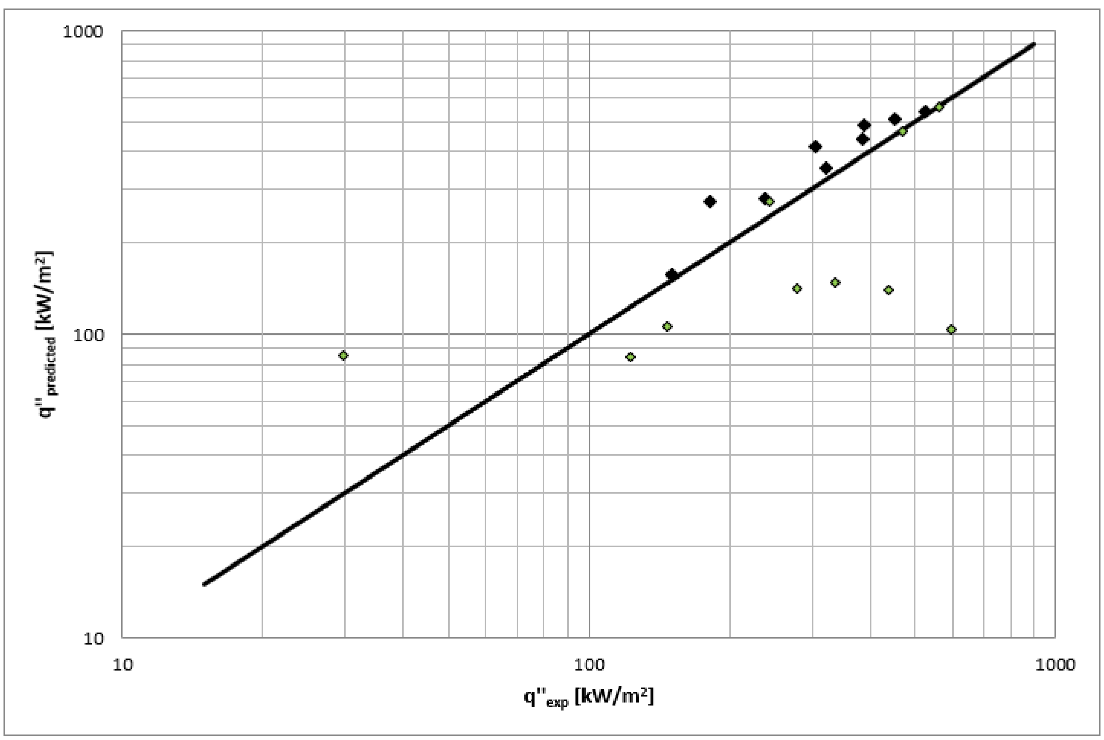

Figure 12: Comparison between LO2 pool burnout points and the CHF correlation of Kandlikar [20]. The solid line is the identity line.

◆ Lyon et al. ◆ Kosky and Lyon

4. FLOW BOILING

Table 7 is a summary of the investigations dealing with flow boiling CHF of LH2. No useful data could be found for flow CHF of LCH4 or LO2.

CHF data was taken from seven experiments for LH2, five of them originating from the same research group. The data of Lewis et al. [38] contained tabulated quality and axial temperature information, so a clear transition from nucleate to film boiling could be easily identified. This transition can also be seen in the data depicted by von Glaun and Lewis [21], which includes both the nucleate and film boiling regimes. The CHF for the remaining sources was estimated from the boiling curve figures in the same manner as discussed earlier for the pool boiling CHF cases. Table 8 shows the statistical results from the six correlations used to predict the flow boiling CHF of LH2, and the individual correlation comparisons can be seen in Figures 13 through 18. The best two correlations are the ones proposed by Shah (Eqs. 19-36) [1] and Katto and Ohno (Eqs. 8-15) [22], both predicting the CHF within a factor two more than 90% of the time.

Based on the 91 data points taken from seven independent sources, it is suggested that the correlation of Katto and Ohno [22] be used to predict the flow CHF of LH2. Katto and Ohno have developed multiple formulations for the CHF, which are fluid property, mass flux, and geometrically dependent. Additionally, their model is divided into two parts, owing to the differences in CHF behavior at higher pressures and fluid density ratios. They also rigorously consider the effect of inlet subcooling. The correlation of Shah [1] also performs well and is therefore recommended.

Table7: Summary of past studies for the flow boiling CHF of LH2.

Reference	Data Type	Boiling Type	Geometry & Orientation	Material	Operating Condition	Additional Comments
von Glaun and Lewis [21]	Plots	Flow nucleate Flow film CHF	Tube (vertical) ID= 14 mm L= 409.6 mm	347 Stainless steel	$2.1 \leq P \leq 4.8$ bar $4.06 \leq G \leq 23.05$ kg/s/m^2 $x \leq 0.93$*	Fluids: LH2, LO2, LN2 *Qualities were not provided by authors but instead computed at temperature sensor locations
Lewis et al. [38]	Plots, Tables	Flow nucleate Flow film CHF	Tube (horizontal) ID= 14.1 mm L= 396.3 mm	304 Stainless steel	$2.1 \leq P \leq 5.4$ bar $3.87 \leq G \leq 95.2$ kg/s/m^2 $x \leq 0.997$	Fluids: LH2, LN2
Shirai et al. [39]	Plots	Flow nucleate Flow film CHF	Tube (vertical) ID=5.95 mm L=100 mm	304 Stainless steel	P= 7 bar G= 75, 260, and 491 kg/s/m^2 $x \leq 0.15$*	Fluids: LH2 *Qualities were not provided by authors but instead computed at the test section center. The wall temperature was assumed to be the arithmetic average of the inlet and outlet wall temperatures.
Tatsumoto et al. [40]	Plots	Flow nucleate Flow film CHF	Tube (horizontal) ID= 3, 6 mm L=100 mm	304 Stainless steel	P= 7 bar G= 270, 948, and 1788 kg/s/m^2 $0.001 \leq x \leq 0.1$*	Fluids: LH2 *Qualities were not provided by authors but instead computed at the test section center. The wall temperature was assumed to be the arithmetic average of the inlet and outlet wall temperatures. DNB correlation proposed
Tatsumoto et al. [41]	Plots	Flow nucleate Flow film CHF	Wire inside center of tube (vertical) D_{wire}= 1.2 mm L_{wire}= 120 mm ID_{tube}= 8 mm	Wire: Pt-Co alloy	P= 7 bar, 11 bar G= 19, 28, 45, 66, 155, and 375 kg/s/m^2 $x \leq 0.7$*	Fluids: LH2 *Qualities were not provided by authors but instead computed at the test section center. The wall temperature was assumed to be the arithmetic average of the inlet and outlet wall temperatures.
Tatsumoto et al. [42]	Plots	Flow nucleate Flow film CHF	Tube (vertical) ID= 4, 6 mm	316 Stainless steel	P= 4 bar, 7 bar G= 86, 146, 167, 187, 207, 302, 327, 336, 656,	Fluids: LH2 *Qualities were not provided by authors but instead computed at the test section center. The

			L= 100, 150, 167, and 250 mm		728, 155, and 375 kg/s/m^2 $x \leq 0.23$*	wall temperature was assumed to be the arithmetic average of the inlet and outlet wall temperatures.
Hartwig et al. [5]	Plots	Flow film	Tube (vertical) ID= 1.02 cm L= 205.6 cm	304 Stainless steel, Pyrex glass	P= 1 bar, 1.4 bar, 2.1 bar, 2.8 bar G= 28, 122, and 441 kg/s/m^2 $x \leq 0.23$*	Fluids: LH2, LN2 *Qualities were not provided by authors but instead computed at the temperature sensor positions. This study involves chill down experiments
Hartwig et al. [6]	Plots	CHF	Tube (vertical) ID= 1.02 cm L= 205.6 cm	304 Stainless steel, Pyrex glass	P= 1 bar, 1.4 bar, 2.1 bar, 2.8 bar G= 28, 122, and 441 kg/s/m^2 $x \leq 0.23$*	Fluids: LH2, LN2 Compared data with the following CHF correlations: Zuber (1959) (pool boiling), Lienhard and Dhir (1973) (pool boiling), Katto and Kurata (1980), Mudawar and Maddox (1990), Katto and Yokoya (1984), This study involves chill down experiments
Yoneda et al. [43]	Plots	Flow nucleate Flow film CHF	Plate on one side of rectangular tube (vertical) W_{duct}= 4.2 mm H_{duct}= 10 mm L_{duct}= 120 mm W_{heater}= 10 mm L_{heater}= 120 mm	Heater Plate: Manganin	P= 7 bar G= 77, 152, and 441 kg/s/m^2 $x \leq 0.12$*	Fluids: LH2 *Qualities were not provided by authors but instead computed at the test section center. The wall temperature was assumed to be the arithmetic average of the inlet and outlet wall temperatures.

Table 8: Mean and standard deviation of ξ, and percentage of experimental data points that fall within a factor of 2.0 and 1.3 of correlations for the flow CHF of LH2

	Shah [1]	Katto [1]	Katto and Ohno [22]	Mudawar and Maddox [5]	Hall and Mudawar [5]	Von Glaun and Lewis [21]
Mean	0.03	0.61	0.00	-0.42	-0.55	0.70
Standard deviation	0.58	2.32	0.44	0.36	0.49	2.15
Percentage of data for which $-0.5 \leq \xi \leq 1.0$	93.41	35.16	91.21	27.47	25.27	31.87
Percentage of data for which $-0.23 \leq \xi \leq 0.3$	48.35	12.09	70.33	17.58	15.38	16.48

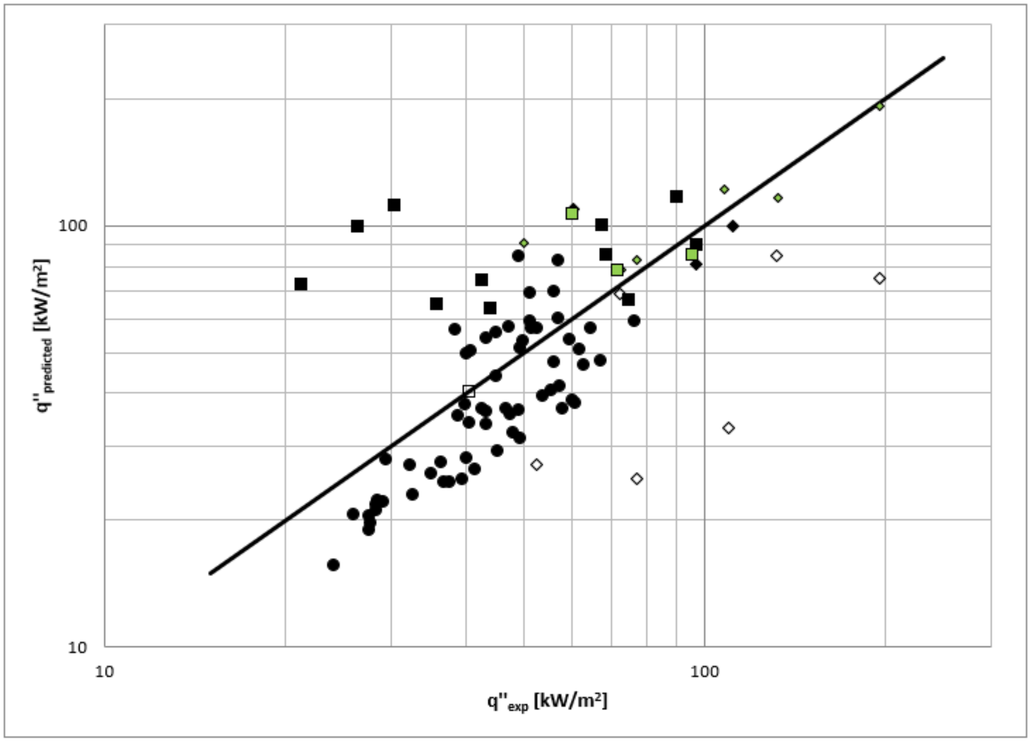

Figure13: Comparison between LH2 flow burnout points and the CHF correlation of Shah [1]. The solid line is the identity line.

◆ Shirai et al. 2011 ◆ Tatsumotoet al. 2012 ◇ Tatsumoto et al. 2014 a ■ Tatsumoto et al. 2014 b

■ Yoneda et al. 2014 □ vonGlaun&Lewis 1960 ● Lewis et al. 1962

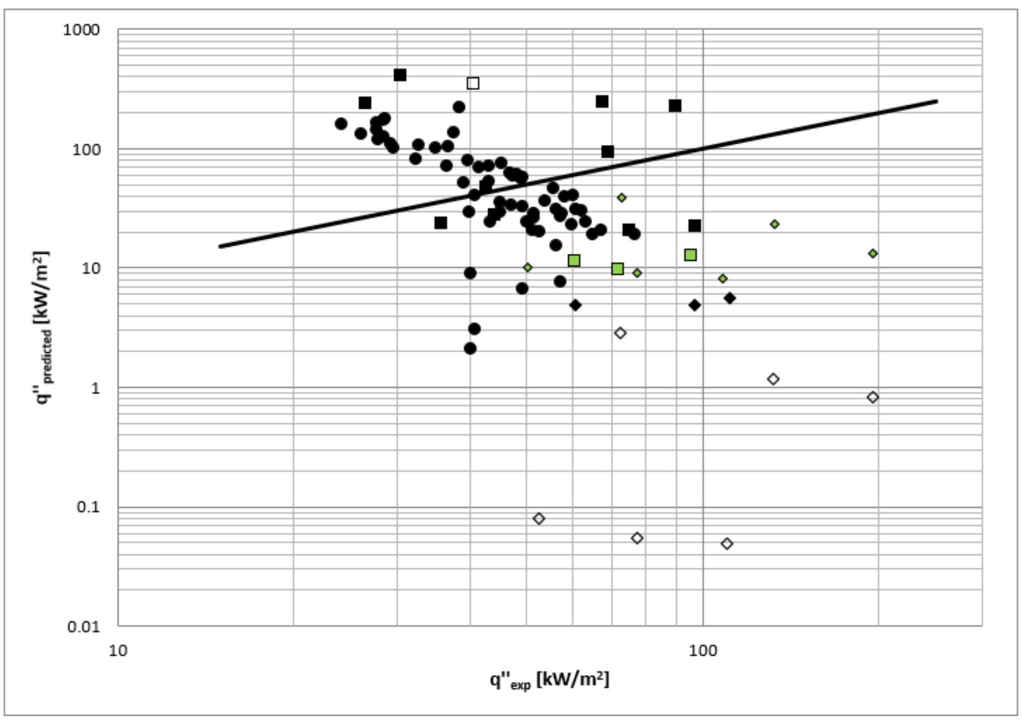

Figure 14: Comparison between LH2 flow burnout points and the CHF correlation of Katto [1]. The solid line is the identity line.

◆ Shirai et al. 2011 ◆ Tatsumotoet al. 2012 ◇ Tatsumoto et al. 2014 a ■ Tatsumoto et al. 2014 b

■ Yoneda et al. 2014 □ vonGlaun&Lewis 1960 ● Lewis et al. 1962

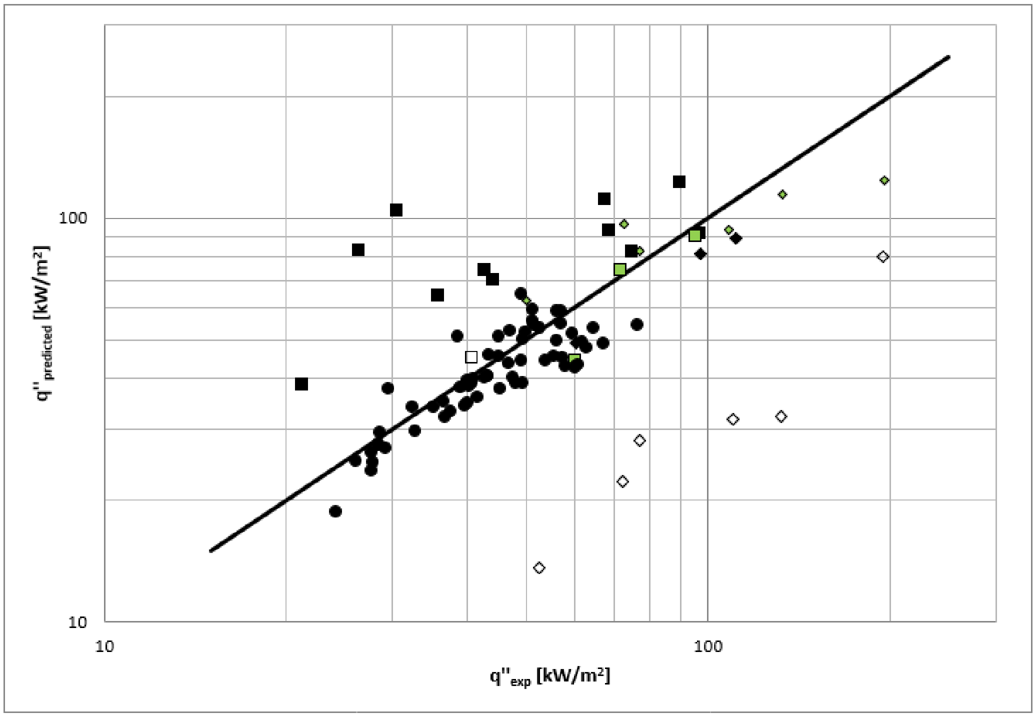

Figure 15: Comparison between LH2 flow burnout points and the CHF correlation of Katto and Ohno [22]. The solid line is the identity line.

◆ Shirai et al. 2011 ◆ Tatsumotoet al. 2012 ◇ Tatsumoto et al. 2014 a ■ Tatsumoto et al. 2014 b

■ Yoneda et al. 2014 □ vonGlaun&Lewis 1960 ● Lewis et al. 1962

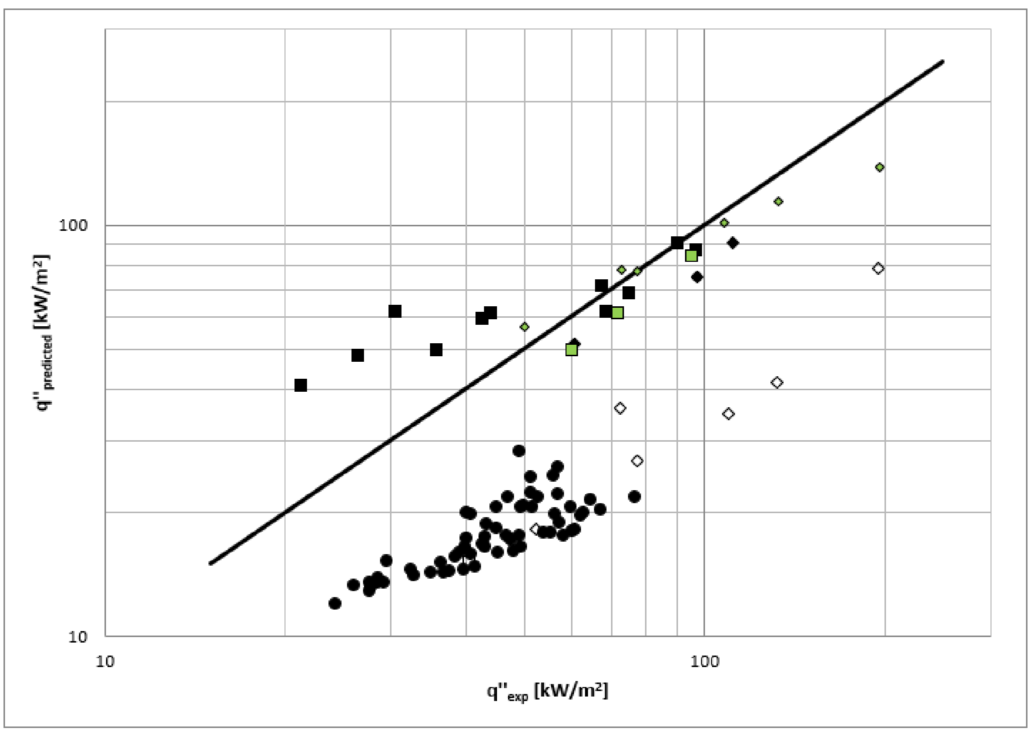

Figure 16: Comparison between LH2 flow burnout points and the CHF correlation of Mudawar and Maddox [5]. The solid line is the identity line.

◆ Shirai et al. 2011 ◆ Tatsumotoet al. 2012 ◇ Tatsumoto et al. 2014 a ■ Tatsumoto et al. 2014 b

■ Yoneda et al. 2014 □ vonGlaun&Lewis 1960 ● Lewis et al. 1962

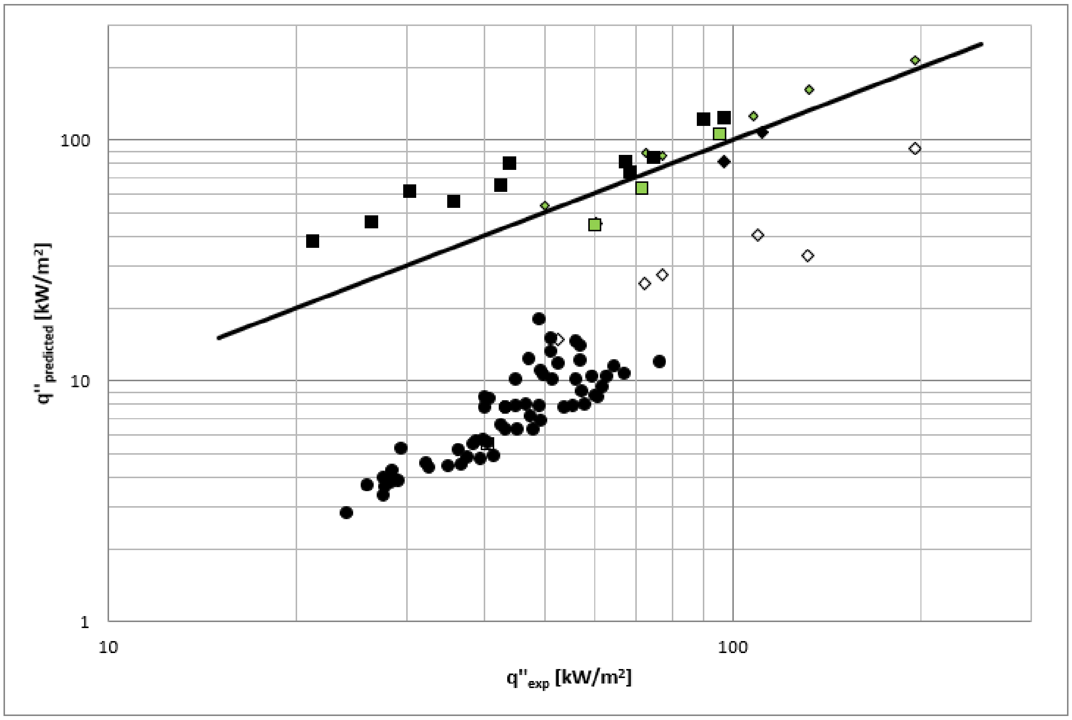

Figure 17: Comparison between LH2 flow burnout points and the CHF correlation of Hall and Mudawar [5]. The solid line is the identity line.

◆ Shirai et al. 2011 ◆ Tatsumotoet al. 2012 ◇ Tatsumoto et al. 2014 a ■ Tatsumoto et al. 2014 b

■ Yoneda et al. 2014 □ vonGlaun&Lewis 1960 ● Lewis et al. 1962

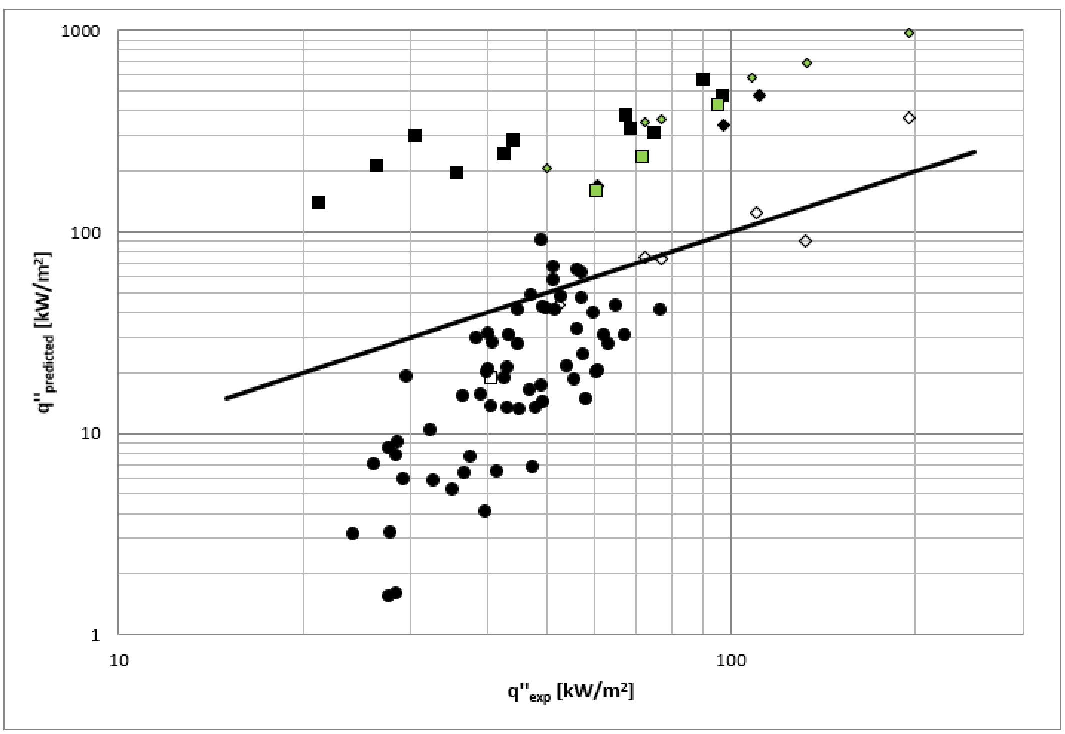

Figure 18: Comparison between LH2 flow burnout points and the CHF correlation of Von Glaun and Lewis [21]. The solid line is the identity line.

◆ Shirai et al. 2011 ◆ Tatsumotoet al. 2012 ◇ Tatsumoto et al. 2014 a ■ Tatsumoto et al. 2014 b

■ Yoneda et al. 2014 □ vonGlaun&Lewis 1960 ● Lewis et al. 1962

CONCLUSIONS

The experimental data available in the open literature for pool and flow boiling CHF of LH2, LCH4 and LO2 were compiled. The compiled data were compared with the predictions of four pool boiling CHF and six flow boiling CHF correlations.

For the pool boiling CHF of LH2 data were extracted from four sources. The correlation of Sun and Lienhard [19] performed best for predicting the CHF and could predict the bulk of the existing heat flux data within an order of magnitude. It could predict 91% of the data within a factor of two.

For the pool boiling CHF of LCH4 data could be found in two sources. The correlation of Lurie and Noyes [18] performed best for predicting the CHF and could predict the bulk of the existing heat flux data within an order of magnitude. It could predict 93% of the data within a factor of two.

For the pool boiling CHF of LO2 data from two sources were used. The correlations of Kandlikar [20] and Sun and Lienhard [19] performed best for predicting the CHF and could predict the bulk of the existing heat flux data within an order of magnitude. They could predict respectively, 79% and 74% of the data within a factor of two.

For the flow boiling CHF of LH2 data were extracted from seven sources. The correlations of Katto and Ohno [22] and Shah [1] performed best for predicting the CHF and could predict the bulk of the existing heat flux data within an order of magnitude. They could predict respectively, 91% and 93% of the data within a factor of two.

No useful data could be found for the flow CHF of LCH4, or LO2.

REFERENCES

[1] S. M. Ghiaasiaan, *Two-Phase Flow, Boiling, and Condensation: In Conventional and Miniature Systems*. Cambridge University Press, 2017.

[2] V. P. Carey, *Liquid vapor phase change phenomena: an introduction to the thermophysics of vaporization and condensation processes in heat transfer equipment*. CRC Press, 2018.

[3] M. R. Baldwin, A. Ghavami, S. Ghiaasiaan, and A. Majumdar, "Pool Boiliing in Liquid Hydrogen, Liquid Methane and Liquid Oxygen: A Review of Available Data and Predictive Tools," *submitted to Cryogenics,* 2020.

[4] M. R. Baldwin, A. Ghavami, S. Ghiaasiaan, and A. Majumdar, "Flow Boiliing in Liquid Hydrogen, Liquid Methane and Liquid Oxygen: A Review of Available Data and Predictive Tools," *submitted to Cryogenics,* 2021.

[5] J. Hartwig, S. Darr, and A. Asencio, "Assessment of existing two phase heat transfer coefficient and critical heat flux correlations for cryogenic flow boiling in pipe quenching experiments," *International Journal of Heat and Mass Transfer,* vol. 93, pp. 441-463, 2016.

[6] J. Hartwig, H. Hu, J. Styborski, and J. Chung, "Comparison of cryogenic flow boiling in liquid nitrogen and liquid hydrogen chilldown experiments," *International Journal of Heat and Mass Transfer,* vol. 88, pp. 662-673, 2015.

[7] I. McDougall, "The boiling of cryogenic fluids—A survey," *Cryogenics,* vol. 11, no. 4, pp. 260-267, 1971.

[8] R. Ahmadi and T. Okawa, "Influence of surface wettability on bubble behavior and void evolution in subcooled flow boiling," *International Journal of Thermal Sciences,* vol. 97, pp. 114-125, 2015.

[9] S. R. Chowdhury and R. Winterton, "Surface effects in pool boiling," *International Journal of Heat and Mass Transfer,* vol. 28, no. 10, pp. 1881-1889, 1985.

[10] V. Dhir and S. Liaw, "Framework for a unified model for nucleate and transition pool boiling," 1989.

[11] B. Bourdon, P. Di Marco, R. Riobóo, M. Marengo, and J. De Coninck, "Enhancing the onset of pool boiling by wettability modification on nanometrically smooth surfaces," *International Communications in Heat and Mass Transfer,* vol. 45, pp. 11-15, 2013.

[12] E. Forrest, E. Williamson, J. Buongiorno, L.-W. Hu, M. Rubner, and R. Cohen, "Augmentation of nucleate boiling heat transfer and critical heat flux using nanoparticle thin-film coatings," *International Journal of Heat and Mass Transfer,* vol. 53, no. 1-3, pp. 58-67, 2010.

[13] J. Bernardin and I. Mudawar, "The Leidenfrost point: experimental study and assessment of existing models," 1999.

[14] T. Bui and V. Dhir, "Transition boiling heat transfer on a vertical surface," 1985.

[15] K. Baumeister and F. Simon, "Leidenfrost temperature—its correlation for liquid metals, cryogens, hydrocarbons, and water," 1973.

[16] N. Zuber, "The hydrodynamic crisis in pool boiling of saturated and subcooled liquids," *Int. Developments in Heat Transfer, ASME,* vol. 27, pp. 230-236, 1961.

[17] S. S. Kutateladze, *Teploperedača pri kondensacii i kipemi*. Masgiz, 1952.

[18] H. Lurie and R. Noyes, *Boiling Studies for Sodium Reactor Safety: Pool boiling and initial forced convection tests and analyses*. Atomics International, 1964.

[19] K.-H. Sun and J. H. Lienhard, "The peak pool boiling heat flux on horizontal cylinders," *International Journal of Heat and Mass Transfer,* vol. 13, no. 9, pp. 1425-1439, 1970.

[20] S. G. Kandlikar, "A theoretical model to predict pool boiling CHF incorporating effects of contact angle and orientation," *J. Heat Transfer,* vol. 123, no. 6, pp. 1071-1079, 2001.

[21] U. von Glahn and J. Lewis, "Nucleate-and Film-Boiling Studies with Liquid Hydrogen," in *Advances in Cryogenic Engineering*: Springer, 1960, pp. 262-269.
[22] Y. Katto and H. Ohno, "An improved version of the generalized correlation of critical heat flux for the forced convective boiling in uniformly heated vertical tubes," *International journal of heat and mass transfer,* vol. 27, no. 9, pp. 1641-1648, 1984.
[23] M. M. Shah, "Improved general correlation for critical heat flux during upflow in uniformly heated vertical tubes," *International Journal of Heat and Fluid Flow,* vol. 8, no. 4, pp. 326-335, 1987.
[24] F. Dittus and L. Boelter, "Heat transfer in automobile radiators of the tubular type," *International Communications in Heat and Mass Transfer,* vol. 12, no. 1, pp. 3-22, 1985.
[25] D. R. Beattie and P. Whalley, "Simple two-phase frictional pressure drop calculation method," *Int. J. Multiphase Flow;(United Kingdom),* vol. 8, no. 1, 1982.
[26] M. R. Baldwin, "Flow and Phase Change Phenomena of Cryogens and Cryogenic Fuels," Georgia Institute of Technology, 2021.
[27] R. N. Mulford and J. P. Nigon, "Heat exchange between a copper surface and liquid hydrogen and nitrogen," Los Alamos Scientific Lab., 1952.
[28] J. Seader, W. S. Miller, and L. Kalvinskas, "Boiling heat transfer for cryogenics," ROCKETDYNE CANOGA PARK CA, 1965.
[29] R. Ehlers, R. Graham, and R. Hendricks, "An experimental study of the pool heating of liquid hydrogen in the subcritical and supercritical pressure regimes over a range of accelerations," 1964.
[30] H. Merte, "Incipient and steady boiling of liquid nitrogen and liquid hydrogen under reduced gravity," 1970.
[31] K. Ohira and H. Furumoto, "Nucleate Pool Boiling Heat Transfer to Slush Hydrogen," in *Proceedings of the Sixteenth International Cryogenic Engineering Conference/International Cryogenic Materials Conference*, 1997: Elsevier, pp. 601-604.
[32] K. Ohira, "Study of nucleate boiling heat transfer to slush hydrogen and slush nitrogen," *Heat Transfer—Asian Research: Co-sponsored by the Society of Chemical Engineers of Japan and the Heat Transfer Division of ASME,* vol. 32, no. 1, pp. 13-28, 2003.
[33] Y. Shirai *et al.*, "Preliminary study on heat transfer characteristics of liquid hydrogen for coolant of HTC superconductors," in *AIP Conference Proceedings*, 2010, vol. 1218, no. 1: AIP, pp. 337-339.
[34] C. Sciance, C. Colver, and C. Sliepcevich, "Pool boiling of methane between atmospheric pressure and the critical pressure," in *Advances in Cryogenic Engineering*: Springer, 1967, pp. 395-408.
[35] P. Kosky and D. Lyon, "Pool boiling heat transfer to cryogenic liquids; I. Nucleate regime data and a test of some nucleate boiling correlations," *AIChE Journal,* vol. 14, no. 3, pp. 372-379, 1968.
[36] D. Lyon, P. Kosky, and B. Harman, "Nucleate boiling heat transfer coefficients and peak nucleate boiling fluxes for pure liquid nitrogen and oxygen on horizontal platinum surfaces from below 0.5 atmosphere to the critical pressures," in *Advances in cryogenic engineering*: Springer, 1964, pp. 77-87.
[37] P. Roubeau, "Heat exchanges in nitrogen and hydrogen boiling under pressure," CEA Saclay, 1961.
[38] J. Goodykoontz, J. Kline, and J. Lewis, "Boiling heat transfer to liquid hydrogen and nitrogen in forced flow," 1962.
[39] Y. Shirai *et al.*, "Forced flow boiling heat transfer of liquid hydrogen for superconductor cooling," *Cryogenics,* vol. 51, no. 6, pp. 295-299, 2011.
[40] H. Tatsumoto *et al.*, "Forced convection heat transfer of subcooled liquid hydrogen in horizontal tubes," in *AIP Conference Proceedings*, 2012, vol. 1434, no. 1: AIP, pp. 747-754.

[41] H. Tatsumoto, Y. Shirai, M. Shiotsu, Y. Naruo, H. Kobayashi, and Y. Inatani, "Forced convection heat transfer from a wire inserted into a vertically-mounted pipe to liquid hydrogen flowing upward," in *Journal of Physics: Conference Series*, 2014, vol. 568, no. 3: IOP Publishing, p. 032017.
[42] H. Tatsumoto *et al.*, "Forced convection heat transfer of saturated liquid hydrogen in vertically-mounted heated pipes," in *AIP Conference Proceedings*, 2014, vol. 1573, no. 1: AIP, pp. 44-51.
[43] K. Yoneda *et al.*, "Forced flow boiling heat transfer properties of liquid hydrogen for manganin plate pasted on one side of a rectangular duct," *Physics Procedia,* vol. 67, pp. 637-642, 2015.